

Continuum Mechanics of a Cellular Tissue Model

Raz Kupferman,^a Ben Maman,^a Michael Moshe^b

^a*Institute of Mathematics, The Hebrew University, Jerusalem 91904, Israel*

^b*The Racah Institute of Physics, The Hebrew University, Jerusalem 91904, Israel*

Abstract

We consider a two-dimensional cellular vertex model, modeling the mechanics of epithelial tissues. The energy of a planar configuration penalizes deviations in each cell from a reference perimeter P_0 and a reference area A_0 . We study the variational limit of this model as the cell size tends to zero, obtaining a continuum variational model. For P_0^2/A_0 below a critical threshold, which corresponds to an isoperimetric constraint, the system is residually-stressed—there are no zero-energy states. For P_0^2/A_0 above this threshold, the zero-energy states are highly degenerate, allowing in particular for the formation of microstructures, which are not captured by formal long-wavelength expansions.

Key words: Cellular models, Γ -convergence, Incompatible elasticity

1 Introduction

Solid mechanics, and in particular the theory of elasticity, was developed originally to describe the statics and the dynamics of inanimate solids and structures. As a consequence, the classical theory does not capture many phenomena occurring in natural and synthetic systems. For example, a fundamental assumption in classical elasticity is the existence of a global stress-free reference configuration. There are, however, solids for which this assumption fails—solids that are residually-stressed even in the absence of external loads. Another class of materials which do not fall within the premises of classical solid mechanics is materials having a degenerate family of stress-free configurations, i.e., materials whose internal structure is non-rigid.

Each of these two classes of materials calls for a different generalization of the theory of elasticity. In the former case, a geometric formulation of elasticity generalizes classical elasticity by assuming the existence of *local* reference

stress-free configurations, quantified in terms of local geometric fields (e.g. a reference metric tensor). Geometric incompatibility emerges when these elements are “sewed” together to form a macroscopic solid. Physical systems with this property are torn plastics [SMS04], self-assembled macro-molecules [AAMS14,ZGDS19], growing solids [Yav10,ZT18] and responsive elastic materials [KES07,KHHS12], to name only a few.

In the latter case, where each element of the structure may acquire multiple local stress-free configurations, a continuum theoretical framework is still not well-established. We emphasize that this class does not include plastic deformations, which transform a material to new reference states via a irreversible deformation. Here, the transition between the multiple reference states is reversible. Inanimate mechanical systems of this type include one- and two-dimensional arrays of rigid elements coupled via hinges and pivots, forming for example origami and kirigami metamaterials, as well as topological mechanics in Maxwell lattices [KL14,CUV14,CLE⁺16, RB17, MES⁺19].

Many of the aforementioned systems that present peculiar mechanics are organic materials [SPM⁺05, DJW05, SLS⁺07]. Moreover, the lack of a unique stress-free configuration is not the only premise that may be violated. For example, a certain class of active solids not conserving mechanical energy was shown to satisfy an anomalous Hooke law, which is not derived from an energy [SSB⁺19]. More generally, the activity of local elements breaks the time reversal symmetry and leads to a rich and complex phenomenology [MJR⁺13].

In this paper, we consider a class of non-rigid systems motivated by the mechanics of *epithelial tissues*. An epithelium is an effectively two-dimensional living cellular tissue, made of cells adhering to each other, leaving no gaps nor voids (confluent phase). Experiments show that epithelia exhibit unusual mechanical properties including glassy dynamics, growth regulation via mechanical stimuli, rigidity transitions, extreme dynamics, and more [AHT⁺10, AHT⁺11, Shr05, NMH⁺17, PKB⁺17], see Figure 1.1. (Experiments on epithelial tissues serve here as a source of inspiration; the model under consideration is not meant to provide a realistic description of such tissues.)

Like for many other biological systems, the mechanics of epithelia were modeled both in the framework of continuum mechanics and in the framework of discrete models. Continuum models have been proposed based on elastic and viscoelastic theories to explain epithelia wrinkled pattern [HPJ11], fold structures [KZ15] and fluidization [RBE⁺10]. These models were not derived from microscopic mechanisms and are therefore purely phenomenological.

On the other hand, there are epithelial vertex models, in which the tissue is modeled as a polygonal tiling of a two-dimensional domain, with each polygon representing a cell. Biological and mechanical properties are encoded in

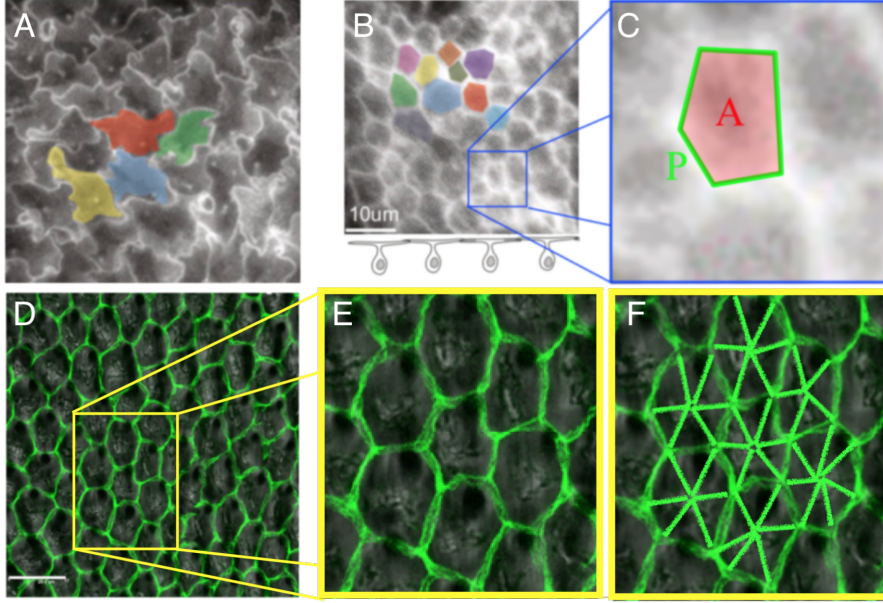


Fig. 1.1. Polygonal modeling of Epithelial tissue. A soft jigsaw phase (A) and a rigid polygonal phase (B) of Trichoplax adherence Epithelial tissue, adopted with permission from Ref. [ABADP18]. Cadherin molecules are distributed along cells' interfaces and induce negative line tension, which is balanced by cell contractility, leading to a preferred cell perimeter P_0 . The preferred three-dimensional shape of each cell as illustrated in bottom of panel (B) is reflected via a preferred cell area A_0 in the two-dimensional effective model. Upon defining the shape parameter $\eta \equiv P_0/\sqrt{A_0}$, the rigid phase in (B) corresponds to small value of η for which no cell can satisfy its reference area and perimeter simultaneously, and a polygonal phase is obtained. An ordered rigid polygonal phase is observed in the Drosophila wing epithelial cells (D,E), adopted with permission from Ref. [CAME05]. An illustration of the triangulation of each cell is shown in (F). The phenomenology of hexagonal (E) and triangular (F) tissue is qualitatively similar, justifying the reduction to the triangular model.

a simplified energy function penalizing each cell for deviations from a *reference area* A_0 and a *reference perimeter* P_0 , encoding microscopic properties as Cadherin molecules concentration and three-dimensional cell geometry [FRA⁺07,SFR⁺10]. This energy, which depends on the network structure and the position of the vertices will be referred to as the *discrete mechanical energy*.

Equilibrium configurations of the cellular model are postulated to be minimizers of the discrete elastic energy [SFR⁺10]. Since living epithelial tissue are in principle out of equilibrium, this assumption is still debatable. Nevertheless, numerical implementations of epithelial vertex models have been used to explain various phenomena, including tissue mechanics, the relation between cell shape and rearrangements in the developing Drosophila embryo [FRA⁺07,SFR⁺10,HTR⁺07] and fluidization in bronchial epithelium [PKB⁺15]. It was observed, in particular, that the dimensionless shape parameter $\eta_0 =$

$P_0/\sqrt{A_0}$ controls a phase transition, which can be interpreted as a transition from a residually-stressed solid to an anomalously-soft phase.

Despite its success, the current study of epithelial vertex models is almost exclusively limited to numerical simulations. A natural question is, whether these vertex models have a continuum limit, and if they do, how do they compare with other continuum models in material science. In the first attempt to study the continuum model of the discrete epithelial vertex model (with uniform hexagonal tiling) it was shown that in the stiff phase the limiting linearized model (in the absence of cell-network remodeling) coincides with elasticity theory of plates and shells [MHK⁺15]. In a more recent work [MBM18], a continuum model for a quasi-static epithelial vertex models with a similar geometry was derived using a formal long-wavelength expansion, and successfully recovered the mechanics of both stiff and soft phases. Its outcome can be viewed as a generalization of incompatible elasticity, where rather than being endowed with one reference metric, the body manifold is endowed with two smooth families of admissible reference metrics.

The goal of this paper is to study rigorously the homogenization problem presented in [MBM18]. For the discrete model, we assume a regular triangular graph of fixed topology (no cell remodeling)—triangles are the most rigid polygons, hence the most convenient to work with. We formulate a family of discrete models parametrized by a parameter $\varepsilon > 0$ representing the linear size of a cell. Using the classical methods of the calculus of variations (e.g., [Dac08,Rin18]), we prove that the discrete models converge, as $\varepsilon \rightarrow 0$, to a limiting continuum model, which like the discrete models, penalizes deviations in area and perimeter.

We show that the shape parameter η_0 controls a transition from a residually-stressed phase to a soft phase. In the soft phase, every state which preserves the reference area and does not increase the reference perimeter has zero energy; the ability to sustain perimeter-shortening deformations at no energetic cost results from the occurrence of microstructures, which are not captured in a formal long-wavelength expansion. Thus, even a triangular lattice model is less rigid than one would naively expect; polygonal models of higher degree are expected to exhibit even more floppiness provided that η_0 is above a critical threshold. Some further directions and some open question are presented in the Discussion.

The analysis presented in this work relies on the theory of the calculus of variations, and specifically on the notion of variational convergence (also known as Γ -convergence). While a research article cannot provide all the required background, we tried to our best to explain all the major steps in the analysis, and interpret the results in a way that is accessible to a broad readership.

2 The discrete cellular model

2.1 Geometric setting

In this section, we present the discrete cellular model. The formulation is cast in a geometric framework, which will facilitate the derivation of the continuum limit.

Let $\Omega \subset \mathbb{R}^2$ be a compact domain with smooth boundary; we denote the Euclidean metric on \mathbb{R}^2 by \mathbf{e} , and use the same notation for the restriction of the Euclidean metric in Ω . The Euclidean metric \mathbf{e} is not viewed here as an intrinsic metric of a solid body; its role is to induce base lengths and areas, with respect to which other lengths and areas are defined. Inner-products and norms with respect to \mathbf{e} are denoted by (\cdot, \cdot) and $|\cdot|$, respectively.

Let $\mathbf{a}, \mathbf{b}, \mathbf{c} \in \mathbb{R}^2$ be unit vectors forming angles of 120 degrees. In particular,

$$\mathbf{a} + \mathbf{b} + \mathbf{c} = 0.$$

For later use, we note that for any linear map $B \in \text{Hom}(\mathbb{R}^2, \mathbb{R}^2)$,

$$|B|^2 = \frac{2}{3} \left(|B(\mathbf{a})|^2 + |B(\mathbf{b})|^2 + |B(\mathbf{c})|^2 \right),$$

where the norm on the left-hand side is the Frobenius norm (i.e., $|B|^2 = \text{Tr}(B^T B)$). Since for every $\alpha, \beta, \gamma \geq 0$, $\alpha^2 + \beta^2 + \gamma^2 \leq (\alpha + \beta + \gamma)^2 \leq 3(\alpha^2 + \beta^2 + \gamma^2)$, it follows that

$$\frac{\sqrt{3}}{\sqrt{2}}|B| \leq |B(\mathbf{a})| + |B(\mathbf{b})| + |B(\mathbf{c})| \leq \frac{3}{\sqrt{2}}|B|. \quad (2.1)$$

Throughout this work, we use the symbols \lesssim and \gtrsim to denote inequalities up to a multiplicative constant, i.e.,

$$f(x) \lesssim g(x)$$

means that there exists a constant $C > 0$ such that $f(x) \leq C g(x)$ for all x . Whenever needed, we will specify on which parameters the multiplicative constant depends. Thus, (2.1) takes the form

$$|B| \lesssim \mathcal{P}(B) \lesssim |B| \quad \text{or} \quad \mathcal{P}(B) \simeq |B|, \quad (2.2)$$

where

$$\mathcal{P}(B) = |B(\mathbf{a})| + |B(\mathbf{b})| + |B(\mathbf{c})| \quad (2.3)$$

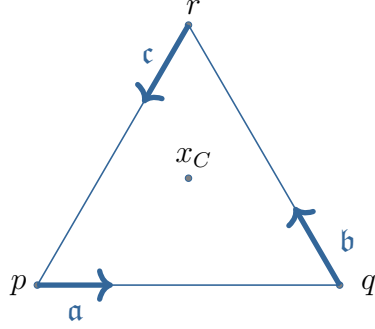


Fig. 2.1. A triangle $t \in T_\varepsilon$.

is the perimeter of an equilateral triangle of unit side length after being deformed by the linear transformation B .

For every $\varepsilon > 0$, let $(V_\varepsilon \subset \Omega, E_\varepsilon)$ be a regular graph forming equilateral triangles of edge length ε . The edges are parallel to the vectors \mathbf{a}, \mathbf{b} and \mathbf{c} . The graph is assumed to be maximal (i.e., cannot be extended without exceeding the boundaries of Ω). Thus, the Hausdorff distance between Ω and V_ε is of order ε (i.e., every point in Ω is at a distance of at most $O(\varepsilon)$ from the nearest point in V_ε).

We denote by T_ε the set of two-dimensional simplexes defined by the graph structure, and by Ω_ε their union; by the maximality of V_ε ,

$$\text{Area}(\Omega \setminus \Omega_\varepsilon) \lesssim \varepsilon.$$

For a triangle $t \in T_\varepsilon$, we denote its barycenter by $x_C(t) \in \Omega_\varepsilon$. We denote its area by

$$\text{Area}_{\text{ref}}(t) = \int_t d\text{Area} = \frac{\sqrt{3}\varepsilon^2}{4}, \quad (2.4)$$

where $d\text{Area}$ is the area form of \mathbf{e} , and we denote by

$$\text{Perim}_{\text{ref}}(t) = 3\varepsilon \quad (2.5)$$

its perimeter.

By construction, if $p, q, r \in \Omega_\varepsilon$ are the vertices of a triangle $t \in T_\varepsilon$, where the segment from p to q is along \mathbf{a} , the segment from q to r is along \mathbf{b} and the segment from r to p is along \mathbf{c} , then

$$q = p + \varepsilon\mathbf{a} \quad r = q + \varepsilon\mathbf{b} \quad \text{and} \quad p = r + \varepsilon\mathbf{c} \quad (2.6)$$

(see Figure 2.1).

2.2 The model

Fix $\varepsilon > 0$. A *discrete configuration* of the cellular structure is a mapping $f_\varepsilon : V_\varepsilon \rightarrow \mathbb{R}^2$. Every discrete configuration f_ε induces distances between the vertices V_ε , and consequently, induces an actual area and actual perimeter on every triangle $t \in T_\varepsilon$. To every discrete configuration f_ε we associate two energy contributions: a *discrete area energy* $E_\varepsilon^A(f_\varepsilon)$ and a *discrete perimeter energy* $E_\varepsilon^P(f_\varepsilon)$, each penalizing for a different form of metric distortion.

The actual (signed) area of a triangle t with vertices p, q, r is given by

$$\text{Area}(t) = \frac{(f_\varepsilon(q) - f_\varepsilon(p)) \wedge (f_\varepsilon(r) - f_\varepsilon(p))}{2 e_1 \wedge e_2}, \quad (2.7)$$

where $\{e_1, e_2\}$ are the standard basis vectors in \mathbb{R}^2 ; the actual perimeter of that triangle is given by

$$\text{Perim}(t) = |f_\varepsilon(q) - f_\varepsilon(p)| + |f_\varepsilon(r) - f_\varepsilon(q)| + |f_\varepsilon(p) - f_\varepsilon(r)|. \quad (2.8)$$

Let A_0 be a smooth positive function on Ω . The *discrete area energy* is of the form

$$E_\varepsilon^A(f_\varepsilon) = \sum_{t \in T_\varepsilon} \Psi \left(\frac{\text{Area}(t)}{A_0(x_C(t)) \text{Area}_{\text{ref}}(t)} \right) \text{Area}_{\text{ref}}(t), \quad (2.9)$$

penalizing deviations of the actual area $\text{Area}(t)$ from the reference area $A_0(x_C(t)) \text{Area}_{\text{ref}}(t)$; the penalty is weighted by the reference area of each triangle. Let $p \geq 2$; the real-valued function Ψ (generally, Ψ may depend on the triangle t) is assumed to satisfy the following conditions:

- (1) Regularity: Ψ is differentiable.
- (2) Positivity: $\Psi \geq 0$, and $\Psi(x) = 0$ if and only if $x = 1$.
- (3) Growth condition:

$$\Psi(x) \lesssim 1 + |x|^{p/2}. \quad (2.10)$$

- (4) Coercivity:

$$\Psi(x) \gtrsim |x - 1|^{p/2} \gtrsim |x|^{p/2} - 1, \quad (2.11)$$

- (5) Lipschitz continuity:

$$|\Psi(x) - \Psi(y)| \lesssim (1 + |x| + |y|)^{p/2-1} |x - y|. \quad (2.12)$$

- (6) Convexity: Ψ is convex.

For example, the function Ψ used in [MBM18] is

$$\Psi(x) = \kappa_A A_0 (x - 1)^2,$$

where κ_A is an elastic constant—the area modulus—and $A_0 = A_0(x_C(t))$. This choice satisfies the required conditions for $p = 4$.

Let P_0 be a smooth positive function on Ω . The *discrete perimeter energy* is of the form

$$E_\varepsilon^P(f_\varepsilon) = \sum_{t \in T_\varepsilon} \Phi \left(\frac{\text{Perim}(t)}{P_0(x_C(t)) \text{Perim}_{\text{ref}}(t)} \right) \text{Area}_{\text{ref}}(t), \quad (2.13)$$

penalizing deviations of the actual perimeter $\text{Perim}(t)$ from the reference perimeter $P_0(x_C(t)) \text{Perim}_{\text{ref}}(t)$; once again, the penalty is weighted by the reference area of each triangle. The function $\Phi : [0, \infty) \rightarrow \mathbb{R}$ satisfies the following requirements:

- (1) Regularity: Φ is differentiable.
- (2) Positivity: $\Phi \geq 0$ and $\Phi(x) = 0$ if and only if $x = 1$.
- (3) Growth condition:

$$\Phi(x) \lesssim 1 + |x|^p. \quad (2.14)$$

- (4) Coercivity:

$$\Phi(x) \gtrsim |x - 1|^p \gtrsim |x|^p - 1. \quad (2.15)$$

- (5) Lipschitz continuity:

$$|\Phi(x) - \Phi(y)| \lesssim (1 + x^{p-1} + y^{p-1})|x - y|. \quad (2.16)$$

- (6) Convexity: Φ is convex.

For example, the function Φ used in [MBM18] is

$$\Phi(x) = \kappa_P P_0(x - 1)^2,$$

where κ_P is another elastic constant—the perimeter modulus—and $P_0 = P_0(x_C(t))$. This choice satisfies the above conditions for $p = 2$.

Finally, the *total discrete energy* is given by

$$E_\varepsilon(f_\varepsilon) = E_\varepsilon^A(f_\varepsilon) + E_\varepsilon^P(f_\varepsilon). \quad (2.17)$$

2.3 Piecewise-affine extension

A discrete configuration $f_\varepsilon : V_\varepsilon \rightarrow \mathbb{R}^2$ can be extended naturally into an \mathbb{R}^2 -valued piecewise-affine function

$$F_\varepsilon : \Omega_\varepsilon \rightarrow \mathbb{R}^2.$$

Specifically, let p , q and r be the vertices of a triangle t as in (2.6). The interior of this triangle can be parameterized as

$$t = \{p + (\alpha \mathbf{a} - \beta \mathbf{c}) : 0 \leq \alpha, \beta, \alpha + \beta \leq \varepsilon\}.$$

We define $F_\varepsilon|_t : t \rightarrow \mathbb{R}^2$ as follows:

$$F_\varepsilon(p + (\alpha \mathbf{a} - \beta \mathbf{c})) = f_\varepsilon(p) + \alpha \frac{f_\varepsilon(q) - f_\varepsilon(p)}{\varepsilon} - \beta \frac{f_\varepsilon(p) - f_\varepsilon(r)}{\varepsilon}.$$

The extension F_ε is affine in the sense that its derivative is piecewise-constant: $dF_\varepsilon|_t : T\Omega|_t \rightarrow \mathbb{R}^2$ is determined by

$$\begin{aligned} dF_\varepsilon(\mathbf{a}) &= \frac{f_\varepsilon(q) - f_\varepsilon(p)}{\varepsilon} \\ dF_\varepsilon(\mathbf{b}) &= \frac{f_\varepsilon(r) - f_\varepsilon(q)}{\varepsilon} \\ dF_\varepsilon(\mathbf{c}) &= \frac{f_\varepsilon(p) - f_\varepsilon(r)}{\varepsilon}. \end{aligned} \tag{2.18}$$

We further extend F_ε into a function $F_\varepsilon \in W^{1,\infty}(\Omega; \mathbb{R}^2)$ such that,

$$\begin{aligned} \|dF_\varepsilon\|_{L^\infty(\Omega; \mathbb{R}^2)} &\lesssim \|dF_\varepsilon\|_{L^\infty(\Omega_\varepsilon; \mathbb{R}^2)} \\ \|dF_\varepsilon\|_{L^p(\Omega; \mathbb{R}^2)} &\lesssim \|dF_\varepsilon\|_{L^p(\Omega_\varepsilon; \mathbb{R}^2)}, \end{aligned} \tag{2.19}$$

where the constant of proportionality is independent of ε . Such a construction is always possible; see [KM18] for details.

The role of the extension $f_\varepsilon \mapsto F_\varepsilon$ is to embed discrete configurations for different values of ε into a common function space. Though purely technical, this construction is key for defining convergence as $\varepsilon \rightarrow 0$.

We next write the discrete energy $E_\varepsilon(f_\varepsilon)$ in terms of the extension F_ε . The actual (signed) area (2.7) of a triangle t can be rewritten as

$$\text{Area}(t) = \int_{F_\varepsilon(t)} d\text{Area} = \int_t \det dF_\varepsilon d\text{Area}. \tag{2.20}$$

Note that $\det dF_\varepsilon$ is constant in t , which implies that

$$\frac{\text{Area}(t)}{\text{Area}_{\text{ref}}(t)} = \det dF_\varepsilon|_t.$$

Denoting by

$$A_{0,\varepsilon} = \sum_{t \in \mathcal{T}_\varepsilon} A_0(x_C(t)) \mathbf{1}_t$$

the piecewise-constant function satisfying $A_{0,\varepsilon}|_t \equiv A_0(x_C(t))$, the discrete area energy (2.9) can be written in integral form:

$$E_\varepsilon^A(f_\varepsilon) = \int_{\Omega_\varepsilon} W_\varepsilon^A(dF_\varepsilon) d\text{Area}, \tag{2.21}$$

where $W_\varepsilon^A : T^*\Omega \otimes \mathbb{R}^2 \rightarrow \mathbb{R}$ is given by

$$W_\varepsilon^A(B) = \Psi \left(\frac{\det B}{A_{0,\varepsilon}} \right). \quad (2.22)$$

The actual perimeter (2.8) of a triangle t with edges p, q, r can be rewritten as

$$\text{Perim}(t) \stackrel{(2.18)}{=} \varepsilon (|dF_\varepsilon(\mathbf{a})| + |dF_\varepsilon(\mathbf{b})| + |dF_\varepsilon(\mathbf{c})|) \stackrel{(2.3)}{=} \varepsilon \mathcal{P}(dF_\varepsilon). \quad (2.23)$$

In view of (2.5),

$$\frac{\text{Perim}(t)}{\text{Perim}_{\text{ref}}(t)} = \frac{\mathcal{P}(dF_\varepsilon)}{3},$$

which is piecewise-constant. Denoting by

$$P_{0,\varepsilon} = \sum_{t \in T_\varepsilon} P_0(x_C(t)) \mathbf{1}_t$$

the piecewise-constant function satisfying $P_{0,\varepsilon}|_t \equiv P_0(x_C(t))$, the discrete perimeter energy (2.13) can be rewritten in integral form,

$$E_\varepsilon^P(f_\varepsilon) = \int_{\Omega_\varepsilon} W_\varepsilon^P(dF_\varepsilon) d\text{Area}, \quad (2.24)$$

where $W_\varepsilon^P : T^*\Omega \otimes \mathbb{R}^2 \rightarrow \mathbb{R}$ is given by

$$W_\varepsilon^P(B) = \Phi \left(\frac{\mathcal{P}(B)}{3P_{0,\varepsilon}} \right). \quad (2.25)$$

Thus, the total discrete energy takes the form

$$E_\varepsilon(f_\varepsilon) = \int_{\Omega_\varepsilon} W_\varepsilon(dF_\varepsilon) d\text{Area}, \quad (2.26)$$

where

$$W_\varepsilon(B) = W_\varepsilon^A(B) + W_\varepsilon^P(B). \quad (2.27)$$

The energy (2.26) is a function of mappings $V_\varepsilon \rightarrow \mathbb{R}^2$. To prepare the grounds for the discrete-to-continuum analysis, we extend E_ε into functionals I_ε on $L^p(\Omega; \mathbb{R}^2)$: For a discrete configuration f_ε we denote its extension by $F_\varepsilon = \iota(f_\varepsilon) \in W^{1,\infty}(\Omega; \mathbb{R}^2)$, which is piecewise-affine on Ω_ε , and denote by $L_\varepsilon^p(\Omega; \mathbb{R}^2) \subset L^p(\Omega; \mathbb{R}^2)$ the image of ι_ε . The functionals

$$I_\varepsilon : L^p(\Omega; \mathbb{R}^2) \rightarrow \mathbb{R} \cup \{\infty\}$$

are given by

$$I_\varepsilon(F) = \begin{cases} \int_{\Omega_\varepsilon} W_\varepsilon(dF) d\text{Area} & F \in L_\varepsilon^p(\Omega; \mathbb{R}^2) \\ \infty & F \in L^p(\Omega; \mathbb{R}^2) \setminus L_\varepsilon^p(\Omega; \mathbb{R}^2). \end{cases} \quad (2.28)$$

3 Gamma convergence

We now study the convergence of the family of functionals I_ε given by (2.28) as $\varepsilon \rightarrow 0$. Define the functional

$$\mathcal{F} : L^p(\Omega; \mathbb{R}) \rightarrow \mathbb{R} \cup \{\infty\}$$

by

$$\mathcal{F}(F) = \begin{cases} \int_{\Omega} QW(dF) d\text{Area} & F \in W^{1,p}(\Omega; \mathbb{R}^2) \\ \infty & F \in L^p(\Omega; \mathbb{R}^2) \setminus W^{1,p}(\Omega; \mathbb{R}^2), \end{cases} \quad (3.1)$$

where for $k \geq 0$ and $p \geq 1$, $W^{k,p}(\Omega; \mathbb{R}^2)$ is the Sobolev space of k -times weakly-differentiable configurations whose derivatives are all in L^p , and

$$W(B) = W^A(B) + W^P(B), \quad (3.2)$$

with

$$W^A(B) = \Psi\left(\frac{\det B}{A_0}\right) \quad \text{and} \quad W^P(B) = \Phi\left(\frac{\mathcal{P}(B)}{3P_0}\right), \quad (3.3)$$

and QW is the quasi-convex envelope of W (i.e., the largest quasi-convex function bounded from above by W) [Dac08, p. 271]. It should be noted that while convexity is a widely-known property, quasi-convexity, which is a weaker condition, is used mostly in the context of variational calculus, where it is a sufficient and necessary condition for the existence of minimizers.

In this section, we prove that I_ε Γ -converges to \mathcal{F} in the $L^p(\Omega; \mathbb{R}^2)$ -topology. The general approach is quite standard: let I_∞ be the Γ -limit of a (not-relabeled) subsequence of I_ε ; such a subsequence exists by the general compactness theorem of Γ -convergence (see Theorem 8.5 in [dal93] for the classical result, or Theorem 4.7 in [KS08] for the case where each functional is defined on a different space). It is sufficient to prove that $I_\infty = \mathcal{F}$. Indeed, since every sequence has a Γ -converging subsequence, the Urysohn property of Γ -convergence (Proposition 8.3 in [dal93]) implies that if all converging subsequences converge to the same limit, then the original sequence converges to that limit.

For the sake of the non-experts in variational calculus, Γ -convergence is the weakest form of convergence for functionals which guarantees that minimizers of functionals in a sequence converge to a minimizer of the limit. Γ -convergence satisfies a compactness property, whereby every sequence of functionals has a converging subsequence. Γ -convergence also satisfies the Urysohn property whereby a sequence converges if and only if there is a unique functional, such as every subsequence has a sub-subsequence converging to it.

3.1 Properties of W_ε and W

We start by establishing a number of properties satisfied by the energy densities W_ε and W , which are all consequences of the properties of Φ and Ψ .

Lemma 3.1 (Uniform coercivity) *The energy densities W_ε and W given by (2.27) and (3.2) are uniformly coercive:*

$$W_\varepsilon(B), W(B) \gtrsim |B|^p - 1, \quad (3.4)$$

where the constant of proportionality does not depend on ε .

Proof: Using the coercivity of Φ ,

$$W_\varepsilon(B) \geq W_\varepsilon^P(B) = \Phi\left(\frac{\mathcal{P}(B)}{3P_{0,\varepsilon}}\right) \stackrel{(2.15)}{\gtrsim} \left(\frac{\mathcal{P}(B)}{3P_{0,\varepsilon}}\right)^p - 1 \stackrel{(2.2)}{\gtrsim} |B|^p - 1,$$

where we used the fact that the infimum of $P_{0,\varepsilon}$ is independent of ε . The proof for W follows the exact same lines. \square

Lemma 3.2 *In two dimensions,*

$$|\det B| \lesssim |B|^2. \quad (3.5)$$

Proof: Using the well-known identity

$$\text{Cof } B B^T = \det B I,$$

and the fact that in two dimensions $|\text{Cof } B| = |B| = |B^T|$,

$$2|\det B| = |\text{Cof } B B^T| \leq |\text{Cof } B||B| = |B|^2. \quad (3.6)$$

\square

Lemma 3.3 (Uniform boundedness) *The energy densities W_ε and W given by (2.27) and (3.2) are uniformly bounded:*

$$W_\varepsilon(B), W(B) \lesssim 1 + |B|^p, \quad (3.7)$$

where the constant of proportionality does not depend on ε .

Proof: By the boundedness of Φ ,

$$W_\varepsilon^P(B) \stackrel{(2.14)}{\lesssim} 1 + \left(\frac{\mathcal{P}(B)}{3P_{0,\varepsilon}} \right)^p \stackrel{(2.2)}{\lesssim} 1 + |B|^p.$$

Likewise, by the boundedness of Ψ ,

$$W_\varepsilon^A(B) \stackrel{(2.10)}{\lesssim} 1 + \left(\frac{|\det B|}{A_{0,\varepsilon}} \right)^{p/2} \stackrel{(3.5)}{\lesssim} 1 + |B|^p.$$

Adding up the two contributions, we obtain the desired result. The same analysis applies for W . \square

Lemma 3.4 *The following inequality holds,*

$$|W(B) - W_\varepsilon(B)| \lesssim \varepsilon(|B| + |B|^p). \quad (3.8)$$

Proof: By the triangle inequality,

$$|W(B) - W_\varepsilon(B)| \leq |W^P(B) - W_\varepsilon^P(B)| + |W^A(B) - W_\varepsilon^A(B)|.$$

By the Lipschitz continuity of Φ ,

$$\begin{aligned} |W^P(B) - W_\varepsilon^P(B)| &= \left| \Phi \left(\frac{\mathcal{P}(B)}{3P_0} \right) - \Phi \left(\frac{\mathcal{P}(B)}{3P_{0,\varepsilon}} \right) \right| \\ &\stackrel{(2.16)}{\lesssim} \left(1 + \left(\frac{\mathcal{P}(B)}{3P_{0,\varepsilon}} \right)^{p-1} + \left(\frac{\mathcal{P}(B)}{3P_0} \right)^{p-1} \right) \left| \frac{\mathcal{P}(B)}{3P_{0,\varepsilon}} - \frac{\mathcal{P}(B)}{3P_0} \right| \\ &\lesssim (\mathcal{P}(B) + (\mathcal{P}(B))^p) \left| \frac{1}{P_{0,\varepsilon}} - \frac{1}{P_0} \right| \\ &\stackrel{(2.2)}{\lesssim} (|B| + |B|^p) \left| \frac{1}{P_{0,\varepsilon}} - \frac{1}{P_0} \right|. \end{aligned}$$

Similarly, by the Lipschitz continuity of Ψ ,

$$\begin{aligned} |W^A(B) - W_\varepsilon^A(B)| &= \left| \Psi \left(\frac{\det B}{A_0} \right) - \Psi \left(\frac{\det B}{A_{0,\varepsilon}} \right) \right| \\ &\stackrel{(2.12)}{\lesssim} \left(1 + \left| \frac{\det B}{A_{0,\varepsilon}} \right|^{p/2-1} + \left| \frac{\det B}{A_0} \right|^{p/2-1} \right) \left| \frac{\det B}{A_{0,\varepsilon}} - \frac{\det B}{A_0} \right| \\ &\lesssim (|\det B| + |\det B|^{p/2}) \left| \frac{1}{A_{0,\varepsilon}} - \frac{1}{A_0} \right| \\ &\stackrel{(3.5)}{\lesssim} (|B|^2 + |B|^p) \left| \frac{1}{A_{0,\varepsilon}} - \frac{1}{A_0} \right|. \end{aligned}$$

Using the fact that

$$\left| \frac{1}{P_{0,\varepsilon}} - \frac{1}{P_0} \right| \lesssim \varepsilon \quad \text{and} \quad \left| \frac{1}{A_{0,\varepsilon}} - \frac{1}{A_0} \right| \lesssim \varepsilon,$$

as well as the fact that $x^2 \leq \max(x, x^p)$, we obtain the desired result. \square

Lemma 3.5 *For every $A, B \in \text{Hom}(\mathbb{R}^2, \mathbb{R}^2)$,*

$$|\det A - \det B| \leq (|A| + |B|)|A - B|. \quad (3.9)$$

Proof: Using again the identity

$$\text{Cof } A A^T = \det A I,$$

we obtain

$$(\det A - \det B)I = \text{Cof } A(A - B)^T + \text{Cof}(A - B)B^T,$$

which together with the fact that $|A| = |A^T| = |\text{Cof } A|$ yields the desired result. \square

Lemma 3.6 *For every $A, B \in T^*\Omega \otimes \mathbb{R}^2$,*

$$|\mathcal{P}(A) - \mathcal{P}(B)| \lesssim |A - B|. \quad (3.10)$$

Proof: We have

$$\begin{aligned} |\mathcal{P}(A) - \mathcal{P}(B)| &= |A(\mathbf{a}) + A(\mathbf{b}) + A(\mathbf{c}) - B(\mathbf{a}) - B(\mathbf{b}) + B(\mathbf{c})| \\ &\leq |A(\mathbf{a}) - B(\mathbf{a})| + |A(\mathbf{b}) - B(\mathbf{b})| + |A(\mathbf{c}) - B(\mathbf{c})| \\ &= \mathcal{P}(A - B) \stackrel{(2.2)}{\lesssim} |A - B|. \end{aligned}$$

\square

Lemma 3.7 *Let $F_\varepsilon \in W^{1,p}(\Omega; \mathbb{R}^2)$ converge to $F \in W^{1,p}(\Omega; \mathbb{R}^2)$ strongly in $W^{1,p}(\Omega; \mathbb{R}^2)$ as $\varepsilon \rightarrow 0$. Then,*

$$\lim_{\varepsilon \rightarrow 0} \int_{\Omega} |W(dF_\varepsilon) - W(dF)| d\text{Area} = 0.$$

Proof: By the Lipschitz continuity of Φ ,

$$\begin{aligned} |W^P(A) - W^P(B)| &\stackrel{(2.16)}{\lesssim} \left(1 + \left(\frac{\mathcal{P}(A)}{3P_0} \right)^{p-1} + \left(\frac{\mathcal{P}(B)}{3P_0} \right)^{p-1} \right) |\mathcal{P}(A) - \mathcal{P}(B)| \\ &\stackrel{(3.10)}{\lesssim} (1 + |A|^{p-1} + |B|^{p-1})|A - B|. \end{aligned}$$

Similarly, by the Lipschitz continuity of Ψ ,

$$\begin{aligned} |W^A(A) - W^A(B)| &\stackrel{(2.12)}{\lesssim} \left(1 + \left(\frac{\det A}{A_0} \right)^{p/2-1} + \left(\frac{\det B}{A_0} \right)^{p/2-1} \right) |\det A - \det B| \\ &\stackrel{(3.9)}{\lesssim} (1 + |A|^{p-2} + |B|^{p-2}) (|A| + |B|) |A - B| \\ &\lesssim (1 + |A|^{p-1} + |B|^{p-1}) |A - B|, \end{aligned}$$

where in the last step we used Young's inequality (i.e., $ab < a^p/p + b^q/q$ for $1/p + 1/q = 1$). Adding the two and using Hölder's inequality (i.e., $\|fg\|_{L^1} = \|f\|_{L^p} \|g\|_{L^q}$ for $1/p + 1/q = 1$),

$$\begin{aligned} \int_{\Omega} |W(dF_{\varepsilon}) - W(dF)| d\text{Area} &\lesssim \left(\text{Area}^{1-1/p}(\Omega) + \|dF_{\varepsilon}\|_{L^p(\Omega; \mathbb{R}^2)}^{p-1} + \|dF\|_{L^p(\Omega; \mathbb{R}^2)}^{p-1} \right) \\ &\quad \times \|dF_{\varepsilon} - dF\|_{L^p(\Omega; \mathbb{R}^2)}, \end{aligned}$$

which converges to zero as $\varepsilon \rightarrow 0$. \square

3.2 Lower and upper bounds

After these preliminaries, we proceed to show that every Γ -limit I_{∞} of I_{ε} equals \mathcal{F} given by (3.1).

Proposition 3.8 (Infinite case) *Let $I_{\infty} : L^p(\Omega; \mathbb{R}^2) \rightarrow \mathbb{R} \cup \{\infty\}$ be a Γ -limit of I_{ε} as $\varepsilon \rightarrow 0$. For every $F \in L^p(\Omega; \mathbb{R}^2) \setminus W^{1,p}(\Omega; \mathbb{R}^2)$,*

$$I_{\infty}(F) = \infty = \mathcal{F}(F).$$

Proof: Assume by contradiction that $I_{\infty}(F) < \infty$. Take a recovery sequence $F_{\varepsilon} \rightarrow F$ in $L^p(\Omega; \mathbb{R}^2)$; without loss of generality, we may assume that the sequence $I_{\varepsilon}(F_{\varepsilon})$ is bounded, and in particular $F_{\varepsilon} \in L_{\varepsilon}^p(\Omega; \mathbb{R}^2)$. Hence,

$$\begin{aligned} 1 &\gtrsim I_{\varepsilon}(F_{\varepsilon}) \\ &= \int_{\Omega_{\varepsilon}} W_{\varepsilon}(dF_{\varepsilon}) d\text{Area} \\ &\stackrel{(3.4)}{\gtrsim} \int_{\Omega_{\varepsilon}} (|dF_{\varepsilon}|^p - 1) d\text{Area} \\ &\gtrsim \|dF_{\varepsilon}\|_{L^p(\Omega_{\varepsilon}; \mathbb{R}^2)}^p - \text{Area}(\Omega) \\ &\stackrel{(2.19)}{\gtrsim} \|dF_{\varepsilon}\|_{L^p(\Omega; \mathbb{R}^2)}^p - \text{Area}(\Omega). \end{aligned}$$

It follows that dF_{ε} is uniformly bounded in L^p . Since F_{ε} converges in $L^p(\Omega; \mathbb{R}^2)$, it is bounded in $W^{1,p}(\Omega; \mathbb{R}^2)$, hence has a convergent subsequence in $W^{1,p}(\Omega; \mathbb{R}^2)$. By the uniqueness of the limit, $F \in W^{1,p}(\Omega; \mathbb{R}^2)$, which contradicts the assumption. \square

Proposition 3.9 (Finite case: lower bound) *Let $I_\infty : L^p(\Omega; \mathbb{R}^2) \rightarrow \mathbb{R} \cup \{\infty\}$ be a Γ -limit of I_ε as $\varepsilon \rightarrow 0$. For every $F \in W^{1,p}(\Omega; \mathbb{R}^2)$,*

$$I_\infty(F) \geq \mathcal{F}(F).$$

Proof: We may assume that $I_\infty(F) < \infty$, otherwise the statement is trivial. Like in the infinite case, we construct a recovery sequence $F_\varepsilon \rightarrow F$ in $L^p(\Omega; \mathbb{R}^2)$, where $F_\varepsilon \in L^p_\varepsilon(\Omega; \mathbb{R}^2)$, and extract a subsequence (not relabeled) that converges to F weakly in $W^{1,p}(\Omega; \mathbb{R}^2)$. Thus, for every $\tilde{\Omega} \subset \Omega$ having positive Hausdorff distance from $\partial\Omega$,

$$\begin{aligned} I_\infty(F) &= \lim_{\varepsilon \rightarrow 0} \int_{\Omega_\varepsilon} W_\varepsilon(dF_\varepsilon) d\text{Area} \\ &\geq \liminf_{\varepsilon \rightarrow 0} \int_{\Omega_\varepsilon} W(dF_\varepsilon) d\text{Area} - \limsup_{\varepsilon \rightarrow 0} \int_{\Omega_\varepsilon} |W_\varepsilon(dF_\varepsilon) - W(dF_\varepsilon)| d\text{Area} \\ &\stackrel{(3.8)}{\gtrsim} \liminf_{\varepsilon \rightarrow 0} \int_{\Omega_\varepsilon} W(dF_\varepsilon) d\text{Area} - \limsup_{\varepsilon \rightarrow 0} \varepsilon \int_{\Omega_\varepsilon} (|dF_\varepsilon| + |dF_\varepsilon|^p) d\text{Area} \\ &\geq \liminf_{\varepsilon \rightarrow 0} \int_{\tilde{\Omega}} W(dF_\varepsilon) d\text{Area} \\ &\geq \liminf_{\varepsilon \rightarrow 0} \int_{\tilde{\Omega}} QW(dF_\varepsilon) d\text{Area} \\ &\geq \int_{\tilde{\Omega}} QW(dF) d\text{Area}. \end{aligned}$$

In the passage to the fourth line we restricted the domain of integration to $\tilde{\Omega}$, which is contained in Ω_ε for small enough ε , and we used the fact that F_ε is uniformly bounded in $W^{1,p}$. In the passage to the fifth line we used the fact that $W \geq QW$. In the passage to the sixth line we used the fact that an integral functional with a quasi-convex integrand is lower-semicontinuous with respect to the weak $W^{1,p}(\Omega; \mathbb{R}^2)$ topology [Dac08, Sect. 8.2]. The proof is complete by letting $\tilde{\Omega} \rightarrow \Omega$, along with dominated convergence. \square

Proposition 3.10 (Upper bound) *Let $I_\infty : L^p(\Omega; \mathbb{R}^2) \rightarrow \mathbb{R} \cup \{\infty\}$ be a Γ -limit of I_ε as $\varepsilon \rightarrow 0$. Then, for every $F \in L^p(\Omega; \mathbb{R}^2)$,*

$$I_\infty(F) \leq \mathcal{F}(F).$$

Proof: If $F \in L^p(\Omega; \mathbb{R}^2) \setminus W^{1,p}(\Omega; \mathbb{R}^2)$, the inequality is trivial because $\mathcal{F}(F) = \infty$ by definition. Let then $F \in W^{1,p}(\Omega; \mathbb{R}^2)$, and take a sequence $F_\varepsilon \in L^p_\varepsilon(\Omega; \mathbb{R}^2)$ converging to F strongly in $W^{1,p}(\Omega; \mathbb{R}^2)$; such a sequence exists by [KM18, Proposition 4.2]. By the lower-semicontinuity of the Γ -limit and by the defi-

inition of $I_\varepsilon(F)$ for $F \in L^p_\varepsilon(\Omega; \mathbb{R}^2)$,

$$\begin{aligned}
I_\infty(F) &\leq \liminf_{\varepsilon \rightarrow 0} I_\varepsilon(F_\varepsilon) \\
&= \liminf_{\varepsilon \rightarrow 0} \int_{\Omega_\varepsilon} W_\varepsilon(dF_\varepsilon) d\text{Area} \\
&\leq \int_\Omega W(dF) d\text{Area} \\
&\quad + \limsup_{\varepsilon \rightarrow 0} \int_\Omega |W_\varepsilon(dF_\varepsilon) - W(dF_\varepsilon)| d\text{Area} \\
&\quad + \limsup_{\varepsilon \rightarrow 0} \int_\Omega |W(dF_\varepsilon) - W(dF)| d\text{Area}.
\end{aligned} \tag{3.11}$$

The second term on the right-hand side vanishes by Lemma 3.4, and the fact that F_ε is uniformly bounded in $W^{1,p}(\Omega; \mathbb{R}^2)$. The third term vanishes by Lemma 3.7.

Thus,

$$I_\infty(F) \leq \int_\Omega W(dF) d\text{Area},$$

and we would be done if we could replace W by QW .

Unfortunately, the inequality between W and QW is in the “wrong” direction. Instead, we proceed by the method used by Le Dret and Raoult [LR95]. We define the functional $J : W^{1,p}(\Omega; \mathbb{R}^2) \rightarrow \mathbb{R}$,

$$J(G) = \int_\Omega W(dG) d\text{Area},$$

and extend it into a functional $\tilde{J} : L^p(\Omega; \mathbb{R}^2) \rightarrow \mathbb{R} \cup \{\infty\}$,

$$\tilde{J}(G) = \begin{cases} J(G) & G \in W^{1,p}(\Omega; \mathbb{R}^2) \\ \infty & G \in L^p(\Omega; \mathbb{R}^2) \setminus W^{1,p}(\Omega; \mathbb{R}^2) \end{cases}.$$

We denote by $\Gamma\tilde{J}$ the lower-semicontinuous envelope of \tilde{J} with respect to the strong L^p topology, and we denote by $\Gamma_w J$ the lower-semicontinuous envelope of J with respect to to weak $W^{1,p}(\Omega; \mathbb{R}^2)$ topology.

Thus, $I_\infty \leq J$ in $W^{1,p}(\Omega; \mathbb{R}^2)$ and therefore $I_\infty \leq \tilde{J}$ in $L^p(\Omega; \mathbb{R}^2)$. Since I_∞ is a Γ limit, it is lower-semicontinuous, therefore

$$I_\infty \leq \Gamma\tilde{J} = \widetilde{\Gamma_w J}$$

where the equality is by [LR95, Lemma 5] (see also [KM18, Prop. 4.6]). In particular, for $F \in W^{1,p}(\Omega; \mathbb{R}^2)$,

$$I_\infty(F) \leq \Gamma_w J(F).$$

But by [AF84] (see also [KM18, Prop. 4.6]),

$$\Gamma_w J(F) = \int_{\Omega} QW(dF) d\text{Area}$$

hence

$$I_{\infty}(F) \leq \int_{\Omega} QW(dF) d\text{Area} = \mathcal{F}(F).$$

□

3.3 Compactness

The last step is to show that every sequence of approximate minimizers of I_{ε} has a subsequence that strongly converges in the strong L^p topology. This, together with the Γ -convergence implies that every sequence of approximate minimizers of I_{ε} has a subsequence converging (modulo a rigid motion) to a minimizer of \mathcal{F} .

Let F_{ε} be a sequence of approximate minimizers, i.e.,

$$\lim_{\varepsilon \rightarrow 0} (I_{\varepsilon}(F_{\varepsilon}) - \inf I_{\varepsilon}) = 0.$$

We first show that the sequence $\inf I_{\varepsilon}$ is bounded: Choose an arbitrary $F \in W^{1,p}(\Omega; \mathbb{R}^2)$, and a recovery sequence φ_{ε} for F . Then,

$$\limsup_{\varepsilon \rightarrow 0} \inf I_{\varepsilon} \leq \lim_{\varepsilon \rightarrow 0} I_{\varepsilon}(\varphi_{\varepsilon}) = \mathcal{F}(F) < \infty$$

Since

$$\lim_{\varepsilon \rightarrow 0} (I_{\varepsilon}(F_{\varepsilon}) - \inf I_{\varepsilon}) = 0,$$

it follows that the sequence $I_{\varepsilon}(F_{\varepsilon})$ is bounded too. Then,

$$\begin{aligned} 1 \gtrsim I_{\varepsilon}(F_{\varepsilon}) &= \int_{\Omega_{\varepsilon}} W_{\varepsilon}(dF_{\varepsilon}) d\text{Area} \\ &\stackrel{(3.4)}{\gtrsim} \int_{\Omega_{\varepsilon}} (|dF_{\varepsilon}|^p - 1) d\text{Area} \gtrsim \|dF_{\varepsilon}\|_{L^p(\Omega; \mathbb{R}^2)}^p - \text{Area}(\Omega), \end{aligned}$$

implying that dF_{ε} is bounded in L^p .

Since we only care about configurations modulo rigid transformations, we may assume without loss of generality, that $\int_{\Omega} F_{\varepsilon} d\text{Area} = 0$. From the Poincaré inequality we deduce that F_{ε} is bounded in $W^{1,p}(\Omega; \mathbb{R}^2)$. It therefore has a weakly converging subsequence in $W^{1,p}$, which by Sobolev embedding strongly converges in L^p .

4 Relation to strain energies

Energies of integral form, where the integrand is a function of the configuration gradient are ubiquitous in elasticity theory. One of the characteristics of an elastic energy density $W : T^*\Omega \otimes \mathbb{R}^2 \rightarrow \mathbb{R}$ is that $W(A) \geq 0$, with $W(A) = 0$ if and only if $A \in T^*\Omega \otimes \mathbb{R}^2$ is an isometry (i.e., preserves lengths and angles). Obviously, for such a clause to have a meaning, Riemannian metrics must be specified for both Ω and \mathbb{R}^2 . For the space manifold \mathbb{R}^2 , the natural metric is the Euclidean one, \mathbf{e} . For the body manifold Ω , one has to explicitly assume the existence of an *intrinsic metric*, so that any linear map $T\Omega \rightarrow \mathbb{R}^2$ can be associated with a notion of deformation, or strain.

In the present context, the manifold Ω is not endowed with an intrinsic metric, but only with intrinsic notions of area and perimeter (recall that the Euclidean metric on Ω has for only role to serve as a reference for area and perimeter). Thus, the energy density W given by (3.2) or its quasi-convex envelope QW are not elastic energy densities. In this section we derive a representation of W as a minimum over elastic energy densities. To this end, we need the following definition:

Definition 4.1 *Let G be a Riemannian metric on Ω . A function $W : T^*\Omega \otimes \mathbb{R}^2 \rightarrow \mathbb{R}$ is called G -elastic if $W \geq 0$ and*

$$W(B) = 0 \quad \text{if and only if} \quad B \in O(G, \mathbf{e}),$$

where $O(G, \mathbf{e})$ denotes the bundle of isometries $(T\Omega, G) \rightarrow (\mathbb{R}^2, \mathbf{e})$ (i.e., the set of pairs (p, A) , where $p \in \Omega$ and $A : T_p\Omega \rightarrow \mathbb{R}^2$ is a linear isometry). It is called orientation-preserving G -elastic if $W \geq 0$ and

$$W(B) = 0 \quad \text{if and only if} \quad B \in SO(G, \mathbf{e}),$$

where $SO(G, \mathbf{e}) \subset O(G, \mathbf{e})$ is the sub-bundle of orientation-preserving isometries (i.e., the set of pairs (p, A) , where $p \in \Omega$ and $A : T_p\Omega \rightarrow \mathbb{R}^2$ is a linear isometry having a positive determinant).

Throughout this section, let

$$\mathbf{u}_1 = \mathbf{a}, \quad \mathbf{u}_2 = \mathbf{b} \quad \text{and} \quad \mathbf{u}_3 = \mathbf{c}.$$

Note that a metric G on Ω is uniquely defined by the three lengths $|\mathbf{u}_i|_G$, $i = 1, 2, 3$, provided that they satisfy the triangle inequality,

$$|\mathbf{u}_i|_G \leq \frac{1}{2} \sum_{i=1}^3 |\mathbf{u}_i|_G \equiv s_G.$$

4.1 The perimeter energy

Definition 4.2 Given the perimeter function P_0 , we denote by $\mathcal{G}[P_0]$ the space of smooth metrics G on Ω satisfying

$$2s_G = \sum_{i=1}^3 |\mathbf{u}_i|_G = 3P_0. \quad (4.1)$$

Proposition 4.3 The perimeter energy density can be represented as

$$W^P(B) = \min_{G \in \mathcal{G}[P_0]} W_G^P(B), \quad (4.2)$$

where

$$W_G^P(B) = \sum_{i=1}^3 \Phi \left(\frac{|B(\mathbf{u}_i)|}{|\mathbf{u}_i|_G} \right) \frac{|\mathbf{u}_i|_G}{2s_G} \quad (4.3)$$

is a G -elastic energy density.

Proof: This is an immediate consequence of the convexity of Φ and Jensen's inequality (i.e., $\Phi(\sum_i p_i x_i) \leq \sum_i p_i \Phi(x_i)$), where p_i are non-negative and sum up to 1): for every $G \in \mathcal{G}[P_0]$, since $2s_G = 3P_0$,

$$W^P(B) = \Phi \left(\sum_{i=1}^3 \frac{|\mathbf{u}_i|_G |B(\mathbf{u}_i)|}{2s_G |\mathbf{u}_i|_G} \right) \leq W_G^P(B).$$

An equality is obtained by choosing G satisfying

$$\frac{|\mathbf{a}|_G}{|B(\mathbf{a})|} = \frac{|\mathbf{b}|_G}{|B(\mathbf{b})|} = \frac{|\mathbf{c}|_G}{|B(\mathbf{c})|}.$$

Note that $|B(\mathbf{a})|$, $|B(\mathbf{b})|$ and $|B(\mathbf{c})|$ satisfy the constraint that the sum of every two is larger than the third, hence so do $|\mathbf{a}|_G$, $|\mathbf{b}|_G$ and $|\mathbf{c}|_G$, thus defining indeed a metric. Finally, $W_G^P(B) = 0$ if and only if $|B(\mathbf{u}_i)| = |\mathbf{u}_i|_G$ for $i = 1, 2, 3$, that is if and only if $B \in \mathcal{O}(G, \mathbf{e})$, proving that W_G^P is G -elastic. \square

4.2 The area energy

A metric G on Ω is also uniquely defined by the quantities,

$$A_G \frac{|\mathbf{a}|_G}{2s_G}, A_G \frac{|\mathbf{b}|_G}{2s_G}, A_G \frac{|\mathbf{c}|_G}{2s_G},$$

where

$$A_G = \sqrt{s_G(s_G - |\mathbf{a}|_G)(s_G - |\mathbf{b}|_G)(s_G - |\mathbf{c}|_G)}$$

is the area of a triangle of edge sizes $|\mathbf{a}|_G$, $|\mathbf{b}|_G$ and $|\mathbf{c}|_G$ (Heron's formula).

Definition 4.4 Given the area function A_0 , we denote by $\mathcal{G}[A_0]$ the space of smooth metrics G on Ω satisfying

$$A_G = \frac{\sqrt{3}}{4} A_0.$$

Note that W^A given by (3.3) can be rewritten as

$$W^A(B) = \Psi \left(\operatorname{sgn}(B) \frac{A_{B^*\epsilon}}{\frac{\sqrt{3}}{4} A_0} \sum_{i=1}^3 \frac{|\mathbf{u}_i|_{B^*\epsilon}}{2s_{B^*\epsilon}} \right). \quad (4.4)$$

where $\operatorname{sgn} B$ is short-hand notation for $\operatorname{sgn}(\det B)$.

Proposition 4.5 The area energy density can be represented as

$$W^A(B) = \min_{G \in \mathcal{G}[A_0]} W_G^A(B), \quad (4.5)$$

where

$$W_G^A(B) = \sum_{i=1}^3 \Psi \left(\frac{\det B \frac{|\mathbf{u}_i|_{B^*\epsilon}}{2s_{B^*\epsilon}}}{A_0 \frac{|\mathbf{u}_i|_G}{2s_G}} \right) \frac{|\mathbf{u}_i|_G}{2s_G}$$

is an orientation-preserving G -elastic energy density.

Proof: We use the convexity of Ψ with Jensen's inequality: for every $G \in \mathcal{G}[A_0]$,

$$W^A(B) = \Psi \left(\sum_{i=1}^3 \frac{|\mathbf{u}_i|_G}{2s_G} \frac{\det B \frac{|\mathbf{u}_i|_{B^*\epsilon}}{2s_{B^*\epsilon}}}{A_0 \frac{|\mathbf{u}_i|_G}{2s_G}} \right) \leq W_G^A(B).$$

An equality is obtained by choosing

$$\frac{|\mathbf{a}|_G}{|B(\mathbf{a})|} = \frac{|\mathbf{b}|_G}{|B(\mathbf{b})|} = \frac{|\mathbf{c}|_G}{|B(\mathbf{c})|},$$

which yields

$$\frac{|\mathbf{a}|_{B^*\epsilon}/2s_{B^*\epsilon}}{|\mathbf{a}|_G/2s_G} = \frac{|\mathbf{b}|_{B^*\epsilon}/2s_{B^*\epsilon}}{|\mathbf{b}|_G/2s_G} = \frac{|\mathbf{c}|_{B^*\epsilon}/2s_{B^*\epsilon}}{|\mathbf{c}|_G/2s_G}.$$

Finally, $W_G^A(B) = 0$ if and only if $|B(\mathbf{u}_i)| = |\mathbf{u}_i|_G$ for $i = 1, 2, 3$ and $\det B > 0$, that is if and only if $B \in \operatorname{SO}(G, \epsilon)$, proving that W_G^A is orientation-preserving G -elastic \square

5 Properties of QW

The explicit calculation of quasi-convex envelopes is a difficult task. This statement is not special to the present work, but ubiquitous in the theory of elas-

ticity. Thus, rather than obtaining an explicit expression for QW , one derives properties that are key in understanding the energetics and the mechanical response of the system. For example, in order to determine how “soft” a system is, it is often sufficient to identify the zero set of QW . Generally, the zero set of QW is larger than the zero set of W , which means that in the continuum limit there may be more zero energy states than suggested when considering the unrelaxed energy density W .

To this end we define the following bundles of maps:

$$\begin{aligned}
\mathcal{K}[P_0] &= \{B \in T^*\Omega \otimes \mathbb{R}^2 : \mathcal{P}(B) = 3P_0\} \\
\mathcal{K}_{\leq}[P_0] &= \{B \in T^*\Omega \otimes \mathbb{R}^2 : \mathcal{P}(B) \leq 3P_0\} \\
\mathcal{K}[A_0] &= \{B \in T^*\Omega \otimes \mathbb{R}^2 : \det B = A_0\} \\
\mathcal{K}[P_0, A_0] &= \mathcal{K}[P_0] \cap \mathcal{K}[A_0] \\
\mathcal{K}_{\leq}[P_0, A_0] &= \mathcal{K}_{\leq}[P_0] \cap \mathcal{K}[A_0].
\end{aligned} \tag{5.1}$$

Note that $W(B) = 0$ if and only if $B \in \mathcal{K}[P_0, A_0]$.

The sets $\mathcal{K}[P_0, A_0]$ and $\mathcal{K}_{\leq}[P_0, A_0]$ are left-SO(2)-invariant, and can be represented in explicit form. Specifically:

Proposition 5.1 *For $\eta_0 = P_0/\sqrt{A_0} \geq 1$,*

$$\mathcal{K}[P_0, A_0] = \text{SO}(2) \times \left\{ \sqrt{A_0} \begin{pmatrix} \alpha \pm \beta(\alpha) \\ 0 & 1/\alpha \end{pmatrix} : \alpha \in [\alpha_{\min}, \alpha_{\max}] \right\},$$

where

$$\beta(\alpha) = (3\eta_0 - \alpha) \frac{\sqrt{\eta_0 \alpha^2 (3\eta_0 - 2\alpha) - 1}}{\sqrt{3\eta_0} \sqrt{3\eta_0 - 2\alpha}},$$

and $\alpha_{\min}, \alpha_{\max}$ are the positive roots of $\eta_0 \alpha^2 (3\eta_0 - 2\alpha) - 1 = 0$. If $\eta_0 = P_0/\sqrt{A_0} < 1$ then

$$\mathcal{K}[P_0, A_0] = \mathcal{K}_{\leq}[P_0, A_0] = \emptyset,$$

corresponding to the isoperimetric inequality for triangles.

Proof: Since $\mathcal{K}[P_0, A_0]$ is left-SO(2)-invariant, any element in that set can be represented in the form

$$\text{SO}(2) \times \sqrt{A_0} \begin{pmatrix} \alpha & \beta \\ 0 & \gamma \end{pmatrix}.$$

The condition on the determinant yields $\gamma = 1/\alpha$. The condition on the

perimeter yields

$$|\alpha| + \left(\left(-\frac{\alpha}{2} + \frac{\sqrt{3}\beta}{2} \right)^2 + \left(\frac{\sqrt{3}}{2\alpha} \right)^2 \right)^{1/2} + \left(\left(\frac{\alpha}{2} + \frac{\sqrt{3}\beta}{2} \right)^2 + \left(\frac{\sqrt{3}}{2\alpha} \right)^2 \right)^{1/2} = \frac{3P_0}{\sqrt{A_0}},$$

from which we extract the two values of β for $\eta_0 > 1$; for $\eta_0 = 1$ the unique solution is $\alpha = 1, \beta = 0$; for $\eta_0 < 1$ there is no solution. \square

By a similar analysis we obtain:

Proposition 5.2 For $P_0/\sqrt{A_0} \geq 1$,

$$\mathcal{K}_{\leq}[P_0, A_0] = \text{SO}(2) \times \left\{ \sqrt{A_0} \begin{pmatrix} \alpha & \gamma \\ 0 & 1/\alpha \end{pmatrix} : \alpha \in [\alpha_{\min}, \alpha_{\max}], |\gamma| \leq \beta(\alpha) \right\}.$$

To proceed to relate W^P, W^A and W to distance from the sets (5.1).

Proposition 5.3 The following inequality holds,

$$W^P(B) \gtrsim \text{dist}^p(B, \mathcal{K}[P_0]).$$

Proof: Suppose that $B \neq 0$ and consider $\tilde{B} \in \mathcal{K}[P_0]$ given by

$$\tilde{B} = \frac{3P_0}{\mathcal{P}(B)} B.$$

Then,

$$\text{dist}^p(B, \mathcal{K}[P_0]) \leq |B - \tilde{B}|^p \simeq \left| \frac{\mathcal{P}(B)}{3P_0} - 1 \right|^p \frac{|B|^p}{(\mathcal{P}(B))^p} \stackrel{(2.15)}{\lesssim} W^P(B).$$

If $B = 0$, then we can perturb it, noting that both sides of the inequality are continuous in B . \square

Proposition 5.4 If $\mathcal{P}(B) > 3P_0$ then $QW(B) > 0$.

Proof: By the previous proposition,

$$W(B) \geq W^P(B) \gtrsim \text{dist}^p(B, \mathcal{K}[P_0]) \geq \text{dist}^p(B, \mathcal{K}_{\leq}[P_0]),$$

where the latter inequality follows from the inclusion $\mathcal{K}[P_0] \subset \mathcal{K}_{\leq}[P_0]$. Since $\mathcal{K}_{\leq}[P_0]$ is a convex set, the function $B \mapsto \text{dist}^p(B, \mathcal{K}_{\leq}[P_0])$ is convex, and in particular quasi-convex, which implies that

$$QW \gtrsim Q\text{dist}^p(\cdot, \mathcal{K}_{\leq}[P_0]) = \text{dist}^p(\cdot, \mathcal{K}_{\leq}[P_0]),$$

and the right-hand side vanishes only if $\mathcal{P}(B) \leq 3P_0$. \square

Proposition 5.5 *If $\det B \neq A_0$ then $QW(B) > 0$.*

Proof: The energy density W^A is poly-convex (i.e., a convex function of the minors of its argument), being a convex function of the determinant, hence it is also quasi-convex [Dac08, Theorem 5.3] (convexity, implies poly-convexity, which implies quasi-convexity, which implies and even weaker form of convexity known as rank-1-convexity); it follows that

$$QW(B) \geq QW^A(B) = W^A(B),$$

and the right-hand side vanishes if and only if $\det B = A_0$, \square

Combining Proposition 5.4 and Proposition 5.5 we obtain:

Corollary 5.6 *If $B \notin \mathcal{K}_{\leq}[P_0, A_0]$ then $QW(B) > 0$.*

We will next show that in fact $QW(B) = 0$ if and only if $B \in \mathcal{K}_{\leq}[P_0, A_0]$.

Proposition 5.7 *The following inequality holds,*

$$W^P(B) \lesssim \text{dist}(B, \mathcal{K}[P_0]) + \text{dist}^p(B, \mathcal{K}[P_0]).$$

Proof: By the Lipschitz continuity of Φ and the fact that $\Phi(1) = 0$,

$$\begin{aligned} W^P(B) &= \left| \Phi \left(\frac{\mathcal{P}(B)}{3P_0} \right) - \Phi(1) \right| \\ &\stackrel{(2.16)}{\lesssim} \left(1 + \left| \frac{\mathcal{P}(B)}{3P_0} \right|^{p-1} \right) \left| \frac{\mathcal{P}(B)}{3P_0} - 1 \right| \\ &\lesssim \left(1 + |\mathcal{P}(B) - 3P_0|^{p-1} \right) |\mathcal{P}(B) - 3P_0|. \end{aligned}$$

Finally, for every $\tilde{B} \in \mathcal{K}[P_0]$,

$$\begin{aligned} |\mathcal{P}(B) - 3P_0| &= |\mathcal{P}(B) - \mathcal{P}(\tilde{B})| \\ &\leq ||B(\mathbf{a})| - |\tilde{B}(\mathbf{a})|| + ||B(\mathbf{b})| - |\tilde{B}(\mathbf{b})|| + ||B(\mathbf{c})| - |\tilde{B}(\mathbf{c})|| \\ &\leq |B(\mathbf{a}) - \tilde{B}(\mathbf{a})| + |B(\mathbf{b}) - \tilde{B}(\mathbf{b})| + |B(\mathbf{c}) - \tilde{B}(\mathbf{c})| \\ &\lesssim |B - \tilde{B}|, \end{aligned}$$

hence

$$|\mathcal{P}(B) - 3P_0| \lesssim \text{dist}(B, \mathcal{K}[P_0]). \quad (5.2)$$

\square

Proposition 5.8 *The following inequality holds,*

$$\begin{aligned} W^A(B) &\lesssim \text{dist}(B, \mathcal{K}[A_0]) + \text{dist}^p(B, \mathcal{K}[A_0]) \\ &\quad + \text{dist}(B, \mathcal{K}[P_0]) + \text{dist}^p(B, \mathcal{K}[P_0]). \end{aligned}$$

Proof: By the Lipschitz continuity of Ψ and the fact that $\Psi(1) = 0$,

$$\begin{aligned} W^P(B) &= \left| \Psi \left(\frac{\det B}{A_0} \right) - \Psi(1) \right| \\ &\stackrel{(2.12)}{\lesssim} \left(1 + \left| \frac{\det B}{A_0} \right|^{p/2-1} \right) \left| \frac{\det B}{A_0} - 1 \right| \\ &\lesssim (1 + |\det B - A_0|^{p/2-1}) |\det B - A_0|. \end{aligned}$$

For every $\tilde{B} \in \mathcal{K}[A_0]$,

$$|\det B - A_0| = |\det B - \det \tilde{B}| \stackrel{(3.5)}{\lesssim} (|B| + |\tilde{B}|) |B - \tilde{B}| \lesssim (|B| + |B - \tilde{B}|) |B - \tilde{B}|,$$

hence

$$|\det B - A_0| \leq |B| \operatorname{dist}(B, \mathcal{K}[A_0]) + \operatorname{dist}^2(B, \mathcal{K}[A_0]).$$

However,

$$|B| \stackrel{(2.2)}{\lesssim} \mathcal{P}(B) \lesssim 1 + |\mathcal{P}(B) - 3P_0| \stackrel{(5.2)}{\lesssim} 1 + \operatorname{dist}(B, \mathcal{K}[P_0]),$$

hence

$$|\det B - A_0| \lesssim \operatorname{dist}(B, \mathcal{K}[A_0]) + \operatorname{dist}^2(B, \mathcal{K}[A_0]) + \operatorname{dist}^2(B, \mathcal{K}[P_0]),$$

and in the last step we used the inequalities $ab \lesssim a^2 + b^2$ and $x^q \lesssim x + x^p$ for every $1 < q < p$. Combining everything we recover the desired result. \square

Combining the last two propositions:

Corollary 5.9 *The following inequality holds,*

$$W(B) \lesssim \operatorname{dist}(B, \mathcal{H}[P_0, A_0]) + \operatorname{dist}^p(B, \mathcal{H}[P_0, A_0]).$$

The set $\mathcal{H}[P_0, A_0]$ is not convex. The calculus of variations literature exhibits various types of convex hull of sets. The *convex hull* K^C of a set K is the smallest convex set containing that set. The *quasi-convex hull* K^{QC} of a set K is defined (there are other equivalent definitions) as the zero set of the related function $Q\operatorname{dist}(\cdot, K)$. Finally, the *laminar convex hull* K^{LC} [Rin18, p. 229] of K is defined recursively as follows,

$$K^{LC} = \bigcup_{i=0}^{\infty} K_i^{LC},$$

where $K_0^{LC} = K$ and for every $i \in \mathbb{N}$,

$$K_{i+1}^{LC} = \{\theta A + (1 - \theta)B : A, B \in K_i^{LC}, \operatorname{rank}(A - B) = 1, \theta \in [0, 1]\}.$$

Theorem 5.10 (Bhattacharya and Dolzmann, [BD01]) *If $K \subset \mathcal{K}[A_0]$ is compact and left-SO(2)-invariant, then*

$$K^{QC} = K^{LC}.$$

(See also [Rin18, p. 239].)

It follows that the zero set of QW is the laminate-convex hull of $\mathcal{K}[P_0, A_0]$. The latter can be calculated rather directly:

Proposition 5.11 *The following equality holds:*

$$(\mathcal{K}[P_0, A_0])^{LC} = \mathcal{K}_{\leq}[P_0, A_0].$$

Proof: If $P_0^2 < A_0$ then both sides are empty. Otherwise, since $\mathcal{K}_{\leq}[P_0]$ is convex, it is closed under convex combinations. Likewise, $\mathcal{K}[A_0]$ is closed under convex combinations of rank-1-connected elements. It follows that

$$(\mathcal{K}[P_0, A_0])^{LC} \subset \mathcal{K}_{\leq}[P_0, A_0].$$

To prove equality, we note that for every $\alpha \in [\alpha_{min}, \alpha_{max}]$,

$$\sqrt{A_0} \begin{pmatrix} \alpha & \beta(\alpha) \\ 0 & 1/\alpha \end{pmatrix} \quad \text{and} \quad \sqrt{A_0} \begin{pmatrix} \alpha & -\beta(\alpha) \\ 0 & 1/\alpha \end{pmatrix},$$

are rank-1-connected, hence for every $\theta \in [0, 1]$,

$$\sqrt{A_0} \begin{pmatrix} \alpha & (2\theta - 1)\beta(\alpha) \\ 0 & 1/\alpha \end{pmatrix} \in (\mathcal{K}[P_0, A_0])_1^{LC},$$

but by Proposition 5.2, every element in $\mathcal{K}_{\leq}[P_0, A_0]$ is of this form. \square

We have thus shown:

Corollary 5.12 *$QW(B) = 0$ if and only if $B \in \mathcal{K}_{\leq}[P_0, A_0]$. In particular, let $P_0^2 \geq A_0$; then, for every*

$$B \in \mathcal{K}_{\leq}[P_0, A_0],$$

the linear map

$$F(x) = Bx$$

is a zero energy state, $\mathcal{F}[F] = 0$.

The fact that the relaxed energy density is insensitive to deformations that shorten the perimeter of triangles can be explained easily. Take for example

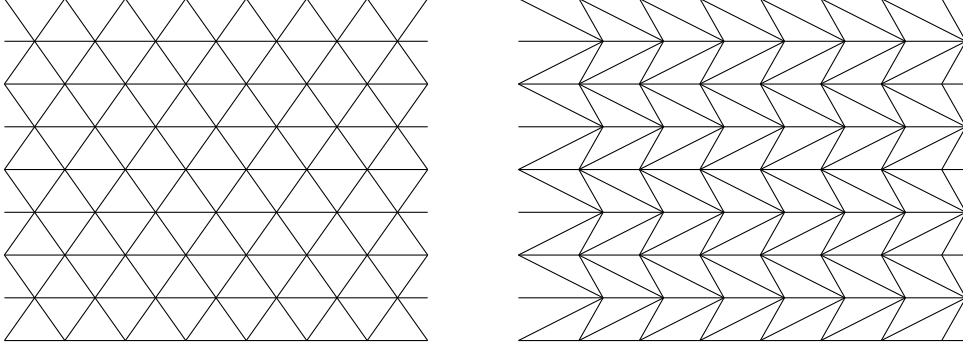


Fig. 5.1. Left: the reference configuration of the lattice. Right: a 1-laminate configuration; each triangle has been deformed to a triangle having the same area and a longer perimeter, such that the boundary of the domain remains (asymptotically, as the discretization is refined) unchanged.

$A_0 = 1$ and $P_0 > 1$ and consider the map $B = \text{Id}$, which is the map for which $\mathcal{P}(B)$ is minimal. That is, $\mathcal{P}(B) = 1 < P_0$, which implies that

$$B \in \mathcal{K}_\pm[P_0, A_0] \setminus \mathcal{K}[P_0, A_0].$$

To illustrate why $QW(B) = 0$, we need to show that a “macroscopic” collection of equilateral triangles can be deformed into triangles having the same area but a longer perimeter, such that the boundary of the domain remains unchanged. The illustration in Figure 5.1 shows how this may occur for any value of $P_0 > 1$. The boundary of the domain can be held constant at the price of violating the area/perimeter constraints along the boundary, which is energetically negligible as the discretization is refined.

6 Isoperimetric obstruction

We have seen that the zero set of QW is the empty set if $A_0 > P_0^2$, which is an *isoperimetric constraint* (i.e., an inequality relating area and perimeter). If A_0 and P_0 fail to satisfy this isoperimetric inequality in some region of Ω , then there are no zero-energy configurations. While this observation follows from the previous section, we can provide a direct proof, which does not rely on advanced results in the calculus of variations:

Proposition 6.1 *Suppose that A_0 and P_0 are smooth and that there exists a point $q \in \Omega$ where*

$$A_0(q) > P_0^2(q).$$

Then,

$$\min_{F \in L^p(\Omega; \mathbb{R}^2)} \mathcal{F}(F) > 0. \quad (6.1)$$

Proof: First, note that the minimum in (6.1) exists because \mathcal{F} is a Γ -limit. We use the property of the Γ limit,

$$\min_{F \in L^p(\Omega; \mathbb{R}^2)} \mathcal{F}(F) = \lim_{\varepsilon \rightarrow 0} \inf_{F_\varepsilon \in L^p_\varepsilon(\Omega; \mathbb{R}^2)} I_\varepsilon(F_\varepsilon) = \lim_{\varepsilon \rightarrow 0} \inf_{f_\varepsilon \in L^p(V_\varepsilon; \mathbb{R}^2)} E_\varepsilon(f_\varepsilon).$$

By the smoothness of A_0 and P_0 , there exist open sets $\Omega'' \subset \Omega' \subset \Omega$ such that

$$A_0 \geq \zeta P_0^2 \quad \text{in } \Omega'$$

for some $\zeta > 1$. Moreover, for ε small enough all triangles $t \in T_\varepsilon$ intersecting Ω'' are contained in Ω' .

Let $t \in T_\varepsilon$ be a triangle intersecting Ω'' . By the isoperimetric inequality for triangles,

$$(\text{Perim}(t))^2 \geq 12\sqrt{3}\text{Area}(t).$$

Since by (2.4) and (2.5),

$$(\text{Perim}_{\text{ref}}(t))^2 = 12\sqrt{3}\text{Area}_{\text{ref}}(t),$$

it follows that

$$\frac{(\text{Perim}(t))^2}{(\text{Perim}_{\text{ref}}(t))^2} \geq \frac{\text{Area}(t)}{\text{Area}_{\text{ref}}(t)},$$

and as $x_C(t) \in \Omega'$,

$$\frac{(\text{Perim}(t))^2}{P_0^2(x_C(t)) (\text{Perim}_{\text{ref}}(t))^2} \geq \zeta \frac{\text{Area}(t)}{A_0(x_C(t)) \text{Area}_{\text{ref}}(t)}.$$

Since Ψ and Φ are continuous and only vanish when their argument is one, there exists a constant $C > 0$ (depending on ζ but not on ε), such that

$$\Psi \left(\frac{\text{Area}(t)}{A_0(x_C(t)) \text{Area}_{\text{ref}}(t)} \right) + \Phi \left(\frac{\text{Perim}(t)}{P_0(x_C(t)) \text{Perim}_{\text{ref}}(t)} \right) \geq C.$$

It follows that for ε small enough and every $f_\varepsilon : V_\varepsilon \rightarrow \mathbb{R}^2$,

$$E_\varepsilon(f_\varepsilon) \geq C \text{Area}(\Omega''),$$

hence

$$\min_{F \in L^p(\Omega; \mathbb{R}^2)} \mathcal{F}(F) \geq C \text{Area}(\Omega'') > 0.$$

□

7 Summary and Discussion

Motivated by the recent growing interest in epithelial vertex models, we derived the continuum limit of a family of discrete models whose energy function penalizes area and perimeter discrepancies. The continuum limit, very

much like the discrete model, penalizes certain area and perimeter deviations from their reference values. When expressed in terms of actual and reference metrics, our continuum vertex model generalizes incompatible-elasticity in that its elastic energy measures metric deviations from two distinct sets of local reference configurations, one representing perimeter constraints and the other representing area constraints. The generalized continuum model exhibits a rigidity transition governed by a ratio between reference values of area and perimeter. The transition is from an elastic-like phase in which area and perimeter are incompatible with each other, to an anomalously soft phase in which area and perimeter are compatible with multiple reference configurations [MBM18]. This transition is consistent with experimental observations on epithelial tissue and with numerical investigations of active epithelial vertex models [PKB⁺15].

While in the present work we focused on a simple prototypical case of triangular network, a future direction is to generalize the analysis to polygons of higher degree and to disordered tilings. We expect the discrete model to converge to an effective continuum model of functional form similar to that obtained in the present work. An open question in this context is whether the rigidity transition described above exists in disordered epithelial vertex models.

An important property of the generalized model is that it forms a unifying framework in which classical elastic solids and cellular tissue are special cases of a more general theory. Classical elasticity corresponds to a single reference configuration associated with each material element, whereas tissue mechanics corresponds to a continuum of reference states associated with each material element. Intermediate cases, e.g., structures with a discrete or a finite number of reference states, form potentially a new type of mechanical metamaterials with properties in between simple solids and biological tissue.

The present work does not account for body forces, surface tractions and other forms of boundary constraints. While “compatible elastostatics” is trivial without forcing or constraints, this is not the case for incompatible systems, which may exhibit non-trivial states also in the absence of constraints. The incorporation of forces to the present model can be done like in other mechanical model; for example, surface tractions are accounted for by adding to the energy a term depending on the displacement of the boundary.

A natural question is the relation between the current rigorous analysis and the long wavelength approximation in [MBM18]. The latter approximation applies in every situation in which the relaxed energy density QW equals the unrelaxed energy density W , i.e., in every situation in which microstructure formation is not energetically favorable. Examples of such situations are tensile boundary conditions; on the other hand, the two models are not equivalent in

the presence of contractive forces.

From a theoretical perspective, the continuum theory derived in this work has the potential to explain observed phenomena. For example, topological transformations of structure networks are fundamental stress-relaxation modes both in elastic solids and in cellular tissue mechanics. However, with no continuum theory in hand, the theoretical analysis of defects in cellular tissue is largely limited. The generalized elastic theory presented in this work opens a new route for theoretical analysis of topological defects in cellular tissue using concepts and tools used for studying topological defects in classical elasticity [MSK15]. Likewise, the continuum model obtained in this work may form a basis for studying some of the classical elastic phenomena, such as waves dynamics, cracks, generalized plates and shells, and more.

Looking forward, we suggest that the relevance of the continuum model goes beyond the scope of cellular tissue mechanics. For example, under-constrained and critically-constrained lattices of harmonic springs, which form the basis for topological mechanics [KL14,CUV14], are structures whose elements have multiple stress-free configurations. Therefore, the technique presented in this paper can in principle be adapted to derive a nonlinear geometric continuum theory of such structures. This will allow, as in the tissue case, to port knowledge from, and to, discrete lattice mechanics and make another step toward a unifying mechanical theory.

Acknowledgments We thank B. Dacorogna, R. Kohn, C. Maor and F. Rindler for helpful advice. We are grateful to S. Armon for illuminating discussions on the mechanics of Trichoplax Adherence. RK was partially funded by the Israel Science Foundation (Grant No. 1035/17). MM was partially funded by the Israel Science Foundation (Grant No. 1441/19).

References

- [AAMS14] S. Armon, H. Aharoni, M. Moshe, and E. Sharon, *Shape selection in chiral ribbons: from seed pods to supramolecular assemblies*, *Soft Matter* **10** (2014), 2733–2740.
- [ABADP18] S. Armon, M.S. Bull, A. Aranda-Diaz, and M. Prakash, *Ultrafast epithelial contractions provide insights into contraction speed limits and tissue integrity*, *Proc. Nat. Acad. Sci. USA* **115** (2018), E10333–E10341.
- [ABS⁺18] L. Atia, D. Bi, Y. Sharma, J.A. Mitchel, B. Gweon, S.A. Koehler, S.J. DeCamp, B. Lan, Kim J.H, R. Hirsch, A.F. Pegoraro, K.H. Lee, J.R. Starr, D.A. Weitz, A.C. Martin, J.-A. Park, J.P. Butler, and J.J. Fredberg, *Geometric constraints during epithelial jamming*, *Nature Phys.* **14** (2018), 613.

- [AF84] E. Acerbi and N. Fusco, *Semicontinuity problems in the calculus of variations*, Arch. Rat. Mech. Anal. **86** (1984), 125–145.
- [AHT⁺10] T.E. Angelini, E. Hannezo, X. Trepate, J.J. Fredberg, and D.A. Weitz, *Cell migration driven by cooperative substrate deformation patterns*, Phys. Rev. Lett. **104** (2010), 168104.
- [AHT⁺11] T.E. Angelini, E. Hannezo, X. Trepate, M. Marquez, J.J. Fredberg, and D.A. Weitz, *Glass-like dynamics of collective cell migration*, Proc. Nat. Acad. Sci. USA **108** (2011), 4714–4719.
- [AP18] S. Armon and M. Prakash, *Ultra fast contractions and emergent dynamics in a living active solid—the epithelium of the primitive animal trichoplax adhaerens*, Biophys. J. **114** (2018), 649.
- [BD01] K. Bhattacharya and G. Dolzmann, *Relaxation of some multi-well problems*, Proc. Roy. Soc. Edinburgh **A131** (2001), 279–320.
- [CAME05] A.-K. Classen, K.I. Anderson, E. Marois, and S. Eaton, *Hexagonal packing of drosophila wing epithelial cells by the planar cell polarity pathway*, Developmental Cell **9** (2005), 805–817.
- [CLE⁺16] B.G. Chen, B. Liu, A.A. Evans, J. Paulose, I. Cohen, V. Vitelli, and C.D. Santangelo, *Topological mechanics of origami and kirigami*, Phys. Rev. Lett. **116** (2016), 135501.
- [CUV14] B.G. Chen, N. Upadhyaya, and V. Vitelli, *Nonlinear conduction via solitons in a topological mechanical insulator*, Proc. Nat. Acad. Sci. USA **111** (2014), 13004–13009.
- [Dac08] B. Dacorogna, *Direct methods in the calculus of variations*, second edition ed., Springer, 2008.
- [dal93] G. dal Maso, *An introduction to Γ -convergence*, Birkhauser, 1993.
- [DJW05] D.E. Discher, P. Janmey, and Y.-L. Wang, *Tissue cells feel and respond to the stiffness of their substrate*, Science **310** (2005), 1139–1143.
- [FRA⁺07] R. Farhadifar, J.-C. Röper, B. Aigouy, S. Eaton, and F. Jülicher, *The influence of cell mechanics, cell-cell interactions, and proliferation on epithelial packing*, Current Biol. **17** (2007), 2095–2104.
- [HPJ11] E. Hannezo, J. Prost, and J.-F. Joanny, *Instabilities of monolayered epithelia: shape and structure of villi and crypts*, Phys. Rev. Lett. **107** (2011), 078104.
- [HTR⁺07] L. Hufnagel, A.A. Teleman, H. Rouault, S.M. Cohen, and B.I. Shraiman, *On the mechanism of wing size determination in fly development*, Proc. Nat. Acad. Sci. USA **104** (2007), 3835–3840.
- [KES07] Y. Klein, E. Efrati, and E. Sharon, *Shaping of elastic sheets by prescription of non-Euclidean metrics*, Science **315** (2007), 1116 – 1120.

- [KHHS12] J. Kim, J.A. Hanna, R.C. Hayward, and C.D. Santangelo, *Thermally responsive rolling of thin gel strips with discrete variations in swelling*, *Soft Matter* **8** (2012), 2375–2381.
- [KL14] C.L. Kane and T.C. Lubensky, *Topological boundary modes in isostatic lattices*, *Nature Phys.* **10** (2014), 39.
- [KM18] R. Kupferman and C. Maor, *Variational convergence of discrete geometrically-incompatible elastic models: II. non-symmetric lattice structures*, *Calc. Var. PDEs* **57** (2018), 39.
- [KS08] K. Kuwae and T. Shioya, *Variational convergence over metric spaces*, *Trans. Amer. Math. Soc.* **360** (2008), 35–75.
- [KZ15] M. Krajnc and P. Ziherl, *Theory of epithelial elasticity*, *Phys. Rev. E* **92** (2015), 052713.
- [LR95] H. Le Dret and A. Raoult, *The nonlinear membrane model as a variational limit of nonlinear three-dimensional elasticity*, *J. Math. Pures Appl.* **74** (1995), 549–578.
- [MBM18] M. Moshe, M.J. Bowick, and M.C. Marchetti, *Geometric frustration and solid-solid transitions in model 2D tissue*, arXiv:1708.07848v4 [cond-mat.soft], 2018.
- [MES⁺19] M. Moshe, E. Esposito, S. Shankar, B. Bircan, I. Cohen, D.R. Nelson, and M.J. Bowick, *Kirigami mechanics as stress relief by elastic charges*, *Phys. Rev. Lett.* **122** (2019), 048001.
- [MHK⁺15] N. Murisic, V. Hakim, I.G. Kevrekidis, S.Y. Shvartsman, and B. Audoly, *From discrete to continuum models of three-dimensional deformations in epithelial sheets*, *Biophys. J.* **109** (2015), 154–163.
- [MJR⁺13] M.C. Marchetti, J.-F. Joanny, S. Ramaswamy, T.B. Liverpool, J. Prost, M. Rao, and R.A. Simha, *Hydrodynamics of soft active matter*, *Rev. Mod. Phys.* **85** (2013), 1143.
- [MSK15] M. Moshe, E. Sharon, and R. Kupferman, *Elastic interactions between two-dimensional geometric defects*, *Phys. Rev. E* **92** (2015), 062403.
- [NMH⁺17] N. Noll, M. Mani, I. Heemskerk, S.J. Streichan, and B.I. Shraiman, *Active tension network model suggests an exotic mechanical state realized in epithelial tissues*, *Nature Phys.* **13** (2017), 1221.
- [PKB⁺15] J.-A. Park, J.H. Kim, D. Bi, J.A. Mitchel, N.T. Qazvini, K. Tantisira, C.Y. Park, M. McGill, S.-H. Kim, B. Gweon, J. Notbohm, R. Steward Jr, S. Burger, S.H. Randell, A.T. Kho, D.T. Tambe, C. Hardin, S.A. Shore, E. Israel, D.A. Weitz, D.J. Tschumperlin, E.P. Henske, S.T. Weiss, M.L. Manning, J.P. Butler, J.M. Drazen, and J.J. Fredberg, *Unjamming and cell shape in the asthmatic airway epithelium*, *Nature. Mat.* **14** (2015), 1040.

- [RB17] A. Rafsanjani and K. Bertoldi, *Buckling-induced kirigami*, Phys. Rev. Lett. **118** (2017), 084301.
- [RBE⁺10] J. Ranft, M. Basan, J. Elgeti, J.-F. Joanny, J. Prost, and F. Jülicher, *Fluidization of tissues by cell division and apoptosis*, Proc. Nat. Acad. Sci. USA **107** (2010), 20863–20868.
- [Rin18] F. Rindler, *Calculus of variations*, Springer, 2018.
- [SFR⁺10] D.B. Staple, R. Farhadifar, J.-C. Röper, B. Aigouy, S. Eaton, and F. Jülicher, *Mechanics and remodelling of cell packings in epithelia*, Eur. Phys. J. E **33** (2010), 117–127.
- [Shr05] B.I. Shraiman, *Mechanical feedback as a possible regulator of tissue growth*, Proc. Nat. Acad. Sci. USA **102** (2005), 3318–3323.
- [SLS⁺07] J. Solon, I. Levental, K. Sengupta, P.C. Georges, and P.A. Janmey, *Fibroblast adaptation and stiffness matching to soft elastic substrates*, Biophys. J. **93** (2007), 4453–4461.
- [SMS04] E. Sharon, M. Marder, and H.L. Swinney, *Leaves, flowers and garbage bags: Making waves*, Amer. Sci. **92** (2004), 254–261.
- [SPM⁺05] C. Storm, J.J. Pastore, F.C. MacKintosh, T.C. Lubensky, and P.A. Janmey, *Nonlinear elasticity in biological gels*, Nature **435** (2005), 191.
- [SSB⁺19] C. Scheibner, A. Souslov, D. Banerjee, P. Surowka, W.T.M. Irvine, and V. Vitelli, *Odd elasticity*, Preprint arXiv 1902.07760, 2019.
- [Yav10] A. Yavari, *A geometric theory of growth mechanics*, J. Nonlinear Sci. **20** (2010), 781–830.
- [ZGDS19] M. Zhang, D. Grossman, D. Danino, and E. Sharon, *Shape and fluctuations of frustrated self-assembled nano ribbons*, Nature communications **10** (2019), 1–7.
- [ZT18] G. Zurlo and L. Truskinovski, *Inelastic surface growth*, Mech. Res. Comm. **93** (2018), 174–179.